Adsorption-desorption kinetics of phosphate between sediment and water in coastal areas

Francoise Andrieux-Loyer, Alain Aminot

Adsorption-desorption kinetics of phosphate between sediment and water in coastal areas.

ANDRIEUX-LOYER Françoise* [1], AMINOT Alain[1]

*Corresponding author: Francoise.Andrieux@ifremer.fr - Phone: (33) 02.98.22.46.77

[1] Ifremer, DYNECO, F-29280 Plouzané, France

ABSTRACT

In this article the kinetics of adsorption-desorption processes of phosphate on sediments is studied according to the Langmuir theory. The theoretical developments are described and applied to the laboratory experiments which rely on desorption of adsorbed phosphate from coastal and estuarine sediments.

Desorption (k_d) and adsorption (k_a and $k_aQ°$) rate constants were determined using sediments from various areas with a wide range of grain size characteristics. Accurate determination of k_d is of primary importance since desorption may directly enhance algal growth. At a temperature of 20 °C, values of k_d range from 0.057 h^{-1} to 0.128 h^{-1}. The results show that the use of k_a, deduced from the Langmuir coefficient b ($b = k_a/k_d$), is not recommended since this coefficient is affected by poor precision. Alternatively, adsorption rates can use the more reliable combined constant $k_aQ°$. Values of k_aQ^o range from 0.013 to 0.054 L g^{-1} h^{-1} (20 °C). The sediment grain size has only moderate influence on the rate constants. The relationship of these rate constants with temperature was studied in the range 1-30°C, encountered in most marine areas. The exponential law with temperature is determined and an increase factor of 1.6 is found for each 10 °C increase. This work has strong implications for environmental modelling to encompass the sediment phase as a contributor to the cycling of essential nutrients in estuarine and coastal systems.

Keywords: exchangeable phosphate, sediment, adsorption, desorption, kinetics.

1. INTRODUCTION

Eutrophication induced by nitrogen and phosphate enrichment in estuarine and coastal areas has been well documented (Boesch, 2002; Seitzinger et al., 2005). Because of the various interactions of phosphate with the solid phase, sediment is a potential phosphate reservoir which may enrich the water column when there is a high demand during intense primary producer growth (Van Raaphorst et al., 1994; Smil, 2000). In oxic coastal and estuarine areas, phosphate concentration is mostly governed by adsorption-desorption of exchangeable phosphate while precipitation and oxidation-reduction of phosphate compounds are mechanisms of minor importance. This most labile phosphate form at the solid-water interface may significantly contribute to the final trophic level of water bodies (Jarvies et al., 2002; Zhang et al., 2012) and induce possible growth of toxic algae.

Models of sediment diagenesis have become essential tools for environmental management by integrating physical, bacteriological and planktonic processes, however adsorbed phosphate generally plays a minor role in these models since it is often included in the iron-bound P fraction (Cha et al., 2005; Ait Ballagh et al., 2020, 2021). In contrast, in coastal waters where eutrophication events are expected, the contribution of exchangeable phosphate is of primary importance as opposed to forms strongly bound to the sediment. Couceiro et al. (2013) showed that by omitting resuspension in a North Sea biochemical model (Baretta et al., 1995) the use of diffusive fluxes of interstitial nutrient concentrations, led to a large underestimation of nutrients concentrations in the water column, and more particularly those of phosphate (from the adsorbed fraction (Sondergaard et al., 1992)). However, sediment-water phosphate exchanges due to the adsorption–desorption process have, until now, been poorly treated because of the unavailability of reliable constants. Up to now, research about phosphate sorption processes has mainly focused on adsorption (Zhou et al., 2005; Wang et al., 2012; Li et al., 2013; Otero et al., 2013; Wang et al., 2022), with little attention towards desorption with the exception of the study of Wang et al (2022). Among these, adsorption constants can generally be found but rarely desorption constants, despite the importance of the sediment phosphate reservoir which may supply the water column.

In a previous article we discussed the determination of the parameters associated with adsorbed phosphate such as the exchangeable phosphate, the partition coefficient and the maximal sediment adsorption capacity using Langmuir's theory as a tool to access this data (Andrieux-Loyer and Aminot, 2023). As the bioavailability of P for phytoplankton depends not only on the quantity of P adsorbed on the sediment but also on the rate of P release, its determination is essential. In this paper the principles of determination of adsorbed phosphate kinetic exchange constants are presented using the Langmuir theory, then applied to the experimental method which are described to obtain these constants. The present work focuses on both desorption and adsorption kinetics

processes from experiments based on phosphate exchange from sediments. First, kinetic constants were established at a temperature of 20 °C, and secondly the temperature dependence of the constants was studied within the range of 1-30 °C most likely encountered in the areas of interest.

2. THEORETICAL CONSIDERATIONS

2.1. Principles of adsorption/desorption processes

The adsorbed phosphate exchange process between sediment and water was previously studied to obtain exchangeable phosphate concentration, partition coefficient and maximal sediment adsorption capacity (Andrieux-Loyer and Aminot, 2023). The Langmuir theory extended from gas to solid-solution interactions by Voice and Weber (1983) was used as a tool to provide these parameters. For kinetics considerations, the solid-water exchange is characterized by adsorption and desorption rates which are treated as first order processes for each reaction component (Voice and Weber, 1983). The Langmuir monolayer adsorption principle is assumed to remain valid given the very low phosphate concentrations in coastal and estuarine waters.

By convention, desorption is treated as a positive rate for the water body, and adsorption as a negative rate. In a given water mass, the phosphate concentration of the solid phase is the product of phosphate on the solid (µmol g^{-1}) and solid in the water (g L^{-1}). So, with the rate constants for desorption and adsorption respectively k_d and k_a:

Desorption rate: $$V_d = \{d([PO_4]_{water})/dt\}_d = k_d[PO_4]_{solid}[solid]_{water} \quad (1)$$

Adsorption rate: $$V_a = -\{d([PO_4]_{water})/dt\}_a = k_a[PO_4]_{water}[free\ sites]_{solid}[solid]_{water} \quad (2)$$

For consistency with previous papers (Aminot and Andrieux, 1996; Andrieux-Loyer and Aminot, 2023), the Langmuir nomenclature was used (Table 1). Phosphate concentrations are symbolised in the water by C (µmol L^{-1}) and on the solid by q (µmol g^{-1}).

125 **Table 1 Nomenclature used herein.**

Variable	symbol	unit
Desorption rate	V_d	µmol L^{-1} h^{-1}
Adsorption rate	V_a	µmol L^{-1} h^{-1}
Desorption constant	k_d	h^{-1}
Adsorption constant	k_a	L µmol^{-1} h^{-1}
Partition coefficient	$K_p = q_e/C_e$	L g^{-1}
Maximal adsorption capacity	Q^o	µmol g^{-1}
Langmuir coefficient	$b = k_a/k_d$	L µmol^{-1}
IN BATCH		
Solution volume	V	L
Solid mass	m	g
Solid concentration	$S = m/V$	g L^{-1}
Initial PO_4 conc. in liquid phase	C_i	µmol L^{-1}
Initial PO_4 conc. on solid (= exchangeable phosphate 'exch-P')	q_i	µmol g^{-1}
PO_4 conc. in liquid phase at time 't'	C_t	µmol L^{-1}
PO_4 conc. on solid at time 't'	q_t	µmol g^{-1}
PO_4 conc. released from solid at time 't'	q_{Rt} (= $q_i - q_t$)	µmol g^{-1}
PO_4 conc. in liquid phase at equilibrium	C_e	µmol L^{-1}
PO_4 conc. on solid at equilibrium	q_e	µmol g^{-1}
PO_4 conc. released from solid at equilibrium	q_{Re} (= $q_i - q_e$)	µmol g^{-1}

126

127 According to the nomenclature, the rates (1) and (2) become:

128 $$V_d = \{dC_t/dt\}_d = k_d q_t S \quad (3)$$

129 $$V_a = -\{dC_t/dt\}_a = -k_a C_t (Q^o - q_t) S \quad (4)$$

130 Solid and water concentrations are stable when the equilibrium is reached ($V_d = V_a$, absolute value), hence:

131

132 $$k_d q_e S = k_a C_e (Q^o - q_e) S \quad (5)$$

133

134 Assuming that $Q°$ exceeds the equilibrium concentration ($Q° >> q_e$), it follows that:

135 $$V_a \approx k_a C_e Q^o S \quad (6)$$

136 and that the partition coefficient at equilibrium is:

137 $$K_p = q_e/C_e = b(Q^o - q_e) \approx bQ^o \quad (7)$$

138

139 The overall treatment of the kinetics data requires first determination of both the exchangeable phosphate
140 (exch-P, symbolised as q_i) and the partition coefficient (K_p), and potentially $Q°$ and b, obtained by the Infinite
141 Dilution Extrapolation (IDE) experiment (Andrieux-Loyer and Aminot, 2023). The rate constants for desorption
142 (k_d) and adsorption (k_a) are obtained by the kinetics batch experiments.

143

2.2. Application to kinetics batch experiments

Batch experiments were performed by adding known masses of sediment to fixed volumes of water of known phosphate concentration. At regular time intervals the concentrations of phosphate in the liquid phase were measured. In this study, focused on phosphate adsorbed on coastal sediments, natural seawater devoid of phosphate (Phosphate-Free Seawater (PFS)) was used for all desorption experiments in order to simplify the computations (Andrieux-Loyer and Aminot, 2023). The low sediment concentrations used in our experiments did not alter the natural seawater pH.

The total exchange rate (equation (3) + (4)) is:

$$V_T = k_a C_t (Q^o - q_t) - k_d q_t = k_a q_{Rt} (m/V)(Q^o - q_i + q_{Rt}) - k_d (q_i - q_{Rt}) \quad (8)$$

Given that V_a and V_d are equal at equilibrium, k_a is expressed as a function of k_d, as follows,

$$k_a q_{Re} (m/V) Q^o = k_d (q_i - q_{Re}) \quad (9)$$

$$k_a = k_d (q_i - q_{Re}) V / q_{Re} m Q^o \quad (10)$$

then k_a is replaced by its value (equation (10)), it comes:

$$V_T = k_d (q_i - q_{Rt}) - k_d (q_i - q_{Re})(q_{Rt}/q_{Re})(Q^o - q_i + q_{Rt})/Q^o \quad (11)$$

With the hypothesis that $Q^o \gg (q_i + q_{Rt})$: $i.e.\ (Q^o - q_i + q_{Rt})/Q^o \approx 1$, equation (11) becomes:

$$V_T = k_d (q_i - q_{Rt}) - k_d (q_i - q_{Re})\, q_{Rt}/q_{Re} \quad (12)$$

Or $$V_T = dq_{Rt}/dt = k_d q_i (q_{Re} - q_{Rt})/q_{re} \quad (13)$$

Thus $$[q_{Re}/(q_{Re} - q_{Rt})] dq_{Rt} = (k_d q_i) dt \quad (14)$$

Integration of equation (14) gives: $$\ln(q_{Re}/(q_{Re} - q_{Rt})) = (k_d q_i / q_{Re}) t \quad (15)$$

The equation (15) may also be written using the the measured equilibrium concentration C_e in the solution:

$$\ln(C_e/(C_e - C_t)) = (k_d q_i S / C_e) t \quad (16)$$

Determination of the desorption rate constant (k_d). Using equation (15) the function $\ln(q_{Re}/(q_{Re} - q_{Rt}))$ is plotted versus time *t*. The desorption rate k_d is calculated from the slope according to

169 $k_d = slope \times (q_{Re}/q_i)$, where q_{Re} is the released phosphate at equilibrium for the kinetics experiment and q_i
170 should have previously been determined by the IDE experiment (Andrieux-Loyer and Aminot, 2023).
171
172 ***Determination of the adsorption rate constants (k_a and $k_aQ°$).*** Ideally the Langmuir coefficient $b = k_a/k_d$ (Table 1) could be obtained from the IDE experiments together with the determination of $Q°$ (equation
174 (18) in Andrieux-Loyer and Aminot, 2023). Then, from the Langmuir coefficient b, the adsorption rate constant
175 k_a is calculated as $k_a = bk_d$. Because b and $Q°$ can not be obtained with a good precision, as previously
176 mentionned (Andrieux-Loyer and Aminot, 2023), we recommend to use the combined constant $k_aQ°$ which can
177 be obtained considering the partition coefficient $K_p = bQ^o$ (equation (7). Thus, using $b = k_a/k_d$, $K_p = k_aQ^o/k_d$
178 and it comes $k_aQ^o = k_dK_p$.

179 # 3. MATERIAL AND METHODS"

180 ## 3.1. Sampling and storage

181 Sediments were sampled in four main French coastal and estuarine areas, with varying types of
182 sediments, over the 1991 – 2005 period (details in Andrieux-Loyer and Aminot, 2023). In addition, four samples
183 were selected from small western France estuaries to enlarge the range of grain size characteristics. The
184 superficial 2 cm layer of the sediments was collected using a Shipek grab. Almost every experiment was carried
185 out immediately on board. When this was not possible, the samples were immediately frozen (-20 °C) in
186 polycarbonate vials for further freeze-drying at the shore laboratory, then sieved at 500 µm before use
187 (Andrieux-Loyer and Aminot, 2023). Similar results were obtained with fresh and lyophilized sediments as
188 shown Fig. 1.

189 ## 3.2. Laboratory experimental procedures

190 ### *3.2.1. Analytical conditions*

191 The concentration of phosphate was determined using Segmented Flow Analysis (SFA; Aminot et al.,
192 2009) with conditions close to those of Murphy and Riley (1962). Precision within series is about 0.005 µmol L^{-1}.

194 Phosphate-Free Seawater (PFS; salinity: 35 ± 0.2) was obtained from coastal seawater collected in late
195 spring, filtered at about 20-50 µm and stored in a non-opaque carboy at ambient light and temperature in the

196 laboratory for a minimum of two months (Aminot et al., 2009). Phosphate, removed by the remaining
197 phytoplankton stays close to the detection level. The water is filtered just before use through Whatman GF/F
198 glass fiber filters (~ 0.7 µm pore size).

199 ***3.2.2. Kinetics experiments***

200 A series of fixed amounts of solid were added to 7-12 flasks containing natural PFS poisoned with
201 mercuric chloride (40 mg L^{-1}) to prevent any biological interference. The sediments amounts were measured
202 using a small calibrated spoon for wet sediments (on-board experiments) and weighted for lyophilyzed
203 sediments. Solid to liquid ratio between 0.2 and 0.6 g L^{-1} were used (constant for each batch). Experiments were
204 performed at 20 °C and the flasks were placed on a shaking table. At predetermined time intervals (up to 50 h),
205 the medium was homogenized then an aliquot was centrifuged (3000 × g, 10 min) and the supernatant was
206 collected and frozen for subsequent phosphate determination. For fresh experiments, sediment remaining after
207 collection of the supernatant was kept for mass determination at the laboratory.

208 From the experimental data, calculation of the rate constant k_d requires the determination of the released
209 phosphate concentration after equilibrium is reached, $q_{Re.}$ According to Voice and Weber (1983), the solid water
210 exchanges are treated as first order processes and therefore, q_{Re}, was computed by a first-order kinetic equation
211 of the TableCurve software (#8143, termed 'Equilibrium concentration').

212 In addition, a study of temperature effect on rate constants was carried out using a sediment from the Bay
213 of Seine (French coast of English Channel), with an exchangeable phosphate concentration of 2.46 µmol g^{-1}
214 (pre-determined using the IDE method). A series of kinetics at 1, 10, 20 and 30 °C was performed by placing the
215 experimental flasks in incubators. Flasks containing PFS were pre-conditioned at the corresponding temperature
216 before addition of the sediment. The samples were manually shaken from time to time and their treatments were
217 similar to those described above for experiments at 20 °C. The duration of experiment was increased to 200 and
218 400 h for 10 °C and 1 °C, respectively.

219 **4. RESULTS**

220 **4.1. Kinetics constants at 20 °C**

221 ***4.1.1. Desorption rate constant***

An example of kinetic experiments performed at 20 °C, in seawater devoid of phosphate is given in Fig. 2A. Desorption of phosphate from sediment was relatively rapid until approaching an apparent equilibrium after about 25 hours.

Data were treated according to the logarithmic equation (15) described in section 2.2 which is illustrated in Fig. 2B. The phosphate concentration released at equilibrium (q_{Re}) was determined according to section 3.2.2 (all fits had $R^2 > 0.93$). The last time points were omitted for the computation due to the high uncertainties caused by the released phosphate approaching q_{Re}. The results are summarized in table 2.

An experiment (sediment S16; table 2) shows that desorption rate constants were very similar regardless of the solid-liquid ratio used. This narrow range of k_d (0.0654 ± 0.004 h^{-1}) at experimental sediment concentrations varying by a factor of 10 confirms that k_d is actually a constant. Overall desorption rates ranged between 0.057 h^{-1} and 0.128 h^{-1} with a mean value of 0.085 ± 0.023 h^{-1} (RSD: 27%).

Table 2 Results of desorption rate constant (k_d) determination obtained from the kinetic experiments according to the function described in Section 2.2.2

Station	S g L^{-1}	n total	n*	R^2	Slope	q_i µmol g^{-1}	q_{Re} µmol g^{-1}	k_d h^{-1}
S16	0.25	7	5	0.976	0.075	2.58	2.20	0.064
S16	0.5	7	5	0.980	0.102	2.58	1.72	0.068
S16	1	7	5	0.975	0.100	2.58	1.55	0.060
S16	2	7	5	0.978	0.126	2.58	1.41	0.069
S3	0.45	7	5	0.976	0.138	1.16	0.97	0.115
S10	0.5	7	4	0.994	0.125	0.74	0.57	0.097
S17	0.2	8	6	0.998	0.140	1.38	1.26	0.128
L23	0.25	7	5	0.983	0.100	5.39	2.99	0.056
G11b	0.5	11	9	0.972	0.090	2.01	1.29	0.058
RA	0.6	12	10	0.901	0.094	3.28	2.70	0.077
B1	0.5	11	7	0.901	0.117	1.64	1.34	0.096
AB	0.6	11	9	0.977	0.106	2.11	1.79	0.088
G7	0.5	8	6	0.870	0.101	1.10	1.00	0.092
B2	0.5	8	5	0.956	0.078	1.30	1.11	0.066

'Total n' is the number of points of the kinetic experiments used to obtain q_{Re} by the asymptotic function. n* is the number of data retained in the application of the logarithmic function for which R^2 and slope are given.

4.1.2. Adsorption rate constants (k_a and $k_aQ°$)

Classically, k_a is the adsorption rate constant of the Langmuir theory which is deduced from the Langmuir coefficient b (= k_a/k_d) and the desorption rate constant k_d previously computed. The coefficient b is determined together with $Q°$ by the Langmuir equations, using the IDE experiment data. However previous studies identified high standard errors for $Q°$, and for its associated coefficient b, when using these equations

(Andrieux-Loyer and Aminot, 2023). A series of b and k_a computed in this way (table 3) illustrate the unrealistically wide range of k_a, spanning 2 orders of magnitude. To overcome the problem of uncertainty of both b and $Q°$, required to obtain the adsorption rates, it is suggested to calculate these rates using the combined constant $k_aQ°$. Indeed, that combined constant is equal to k_dK_p, knowing that K_p is easily obtained from the IDE experiment data with an acceptable precision (Andrieux-Loyer and Aminot, 2023). Results are shown in Table 3. The range of the combined constant is rather narrow, 0.013 to 0.054 L g^{-1}, with a mean value of 0.028 L g^{-1} (s: 0.011; RSD: ± 38%).

Table 3 Results of adsorption rate constants (k_a and $k_aQ°$) determinations.

Station	k_d h^{-1}	b L µmol^{-1}	$k_a = bk_d$ L µmol^{-1} h^{-1}	K_p L g^{-1}	$k_aQ° = k_dK_p$ L g^{-1} h^{-1}
S16 (mean)	0.065	0.37	0.024	0.20	0.013
S3	0.115	0.93	0.108	0.21	0.024
S10	0.097	0.73	0.071	0.25	0.024
S17	0.128	0.62	0.079	0.42	0.054
L23	0.056	0.016	0.0009	0.31	0.017
G11b	0.058	0.79	0.046	0.64	0.037
RA	0.077	0.050	0.004	0.31	0.024
B1	0.096	0.36	0.034	0.35	0.033
AB	0.088	0.36	0.032	0.34	0.030
G7	0.092	-	-	0.26	0.024
B2	0.066	0.28	0.019	0.49	0.033

4.1.3 Salinity effect on rate constants

Although eutrophication occurs only in low turbid outer estuaries, in coastal waters of high salinity, an experiment was performed with a sediment similar to L23 to compare desorption constants k_d in two extreme conditions, sea water and pure demineralized water. The measured k_d of 0.071 and 0.105 h^{-1}, respectively, remain within the range of constants obtained for all the sediments tested in this study (section 4.1.1), which shows that the effect of salinity on desorption rates over the whole salinity range is not significant. In coastal waters this effect will be negligible. Regarding the adsorption constant k_aQ°, which is a function of the partition coefficient K_p ($k_aQ^{\circ} = k_dK_p$; section 2.2), a slight effect may be expected which will depend on the nature of the fresh water used (dissolved ions and pH). However, within the range of values obtained in the various sediments tested (see Table 5) this effect is likely insignificant in the coastal areas subject to eutrophication events.

4.2. Temperature effect on rate constants

4.2.1. Comparison of released concentration

Phosphate release from the sediment at various temperatures is provided in Figure 3. Before further computation of rate constants, the effect of temperature on the amount of phosphate released at equilibrium has been examined.

Table 4 shows that final equilibrium concentrations lie between 2.13 and 2.20 µmol g^{-1} within the temperature range while the computed q_{Re} lies between 2.06 and 2.22 µmol g^{-1}. Within the determined uncertainty of about ± 2-4 percent, the equilibrium values are not significantly different at the 95% confidence level. Such variability appears consistent in experiments requiring multiple weighing of heterogeneous material such as sediments. Consequently, the equilibrium concentration can be assumed to be independent of temperature in the range 1-30 °C for most purposes.

Table 4. Final and computed equilibrium concentrations at the various temperatures.

Temperature	**1 °C**	**10 °C**	**20 °C**	**30 °C**
Maximum experiment time	400 h	200 h	50 h	30 h
Final PO_4 measured value µmol g^{-1}	2.15	2.13	2.19	2.20
Computed equilibrium PO_4 (q_{Re}) µmol g^{-1}	2.06	2.10	2.22	2.15
standard error	*0.05*	*0.05*	*0.09*	*0.05*

The partition coefficient K_p is required for the determination of the adsorption rate constant. It is computed as $K_p = q_e/C_e$ (see Table 1), with $q_e = q_i - q_{Re}$ and $C_e = q_{Re} \times S$. Since every term is constant K_p is independent of temperature in the 1-30 °C range. This result indicates that all K_p determined at 20 °C (Andrieux-Loyer and Aminot, 2023) are valid regardless of the temperature encountered in most coastal environments. In the present experiments, the reference value of q_{Re} was taken as the average of the equilibrium values at 20 and 30 °C (2.18 µmol g^{-1}), to avoid a risk that slightly lower values at 1 and 10 °C might result from potentially too short experimental durations. Hence, with q_i = 2.46 µmol g^{-1}, q_{Re} = 2.18 µmol g^{-1} and S = 0.25 g L^1, one obtained K_p = 0.514 L g^{-1}.

The so-called Langmuir coefficient b ($b = k_a/k_d$) is linked to K_p by the relation $K_p = b(Q°-q_e)$. Since K_p, $Q°$ (maximum adsorption capacity) and q_e are constant, b is also constant in the temperature range 1-30°C. Consequently, the two rate constants k_a and k_d show similar variations in relation to temperature so that their ratio is independent of temperature.

4.2.2 Determination of temperature effect on rate constants

The logarithmic function, which enables the computation of k_d, includes the difference between q_{Re} and PO_4 released at any times. The q_{Re} value of 2.18 µmol g^{-1} previously used for the determination of K_p, was also used in the computation of k_d (section 4.2.2). Since q_{Re} exhibits an uncertainty of a few percents, experimental data too close to q_{Re} were omitted to improve the precision. Consequently, only the 5-6 measures of PO_4 released up to 20 hours were considered for computation. The results are illustrated in Fig. 4A and summarized in table 5.

Table 5 Results of rate constants (k_d, k_a and $k_aQ°$) obtained at various temperatures. Common main data: S = 0.25 g L^{-1}; q_i (= exch-P) = 2.46 µmol g^{-1}; q_{Re} = 2.18 µmol g^{-1}; K_p = 0.514 L g^{-1}.

	ln function			
Temperature °C	**R^2**	**Slope**	**k_d** h^{-1}	**$k_aQ° = k_dK_p$** L g^{-1} h^{-1}
1	0.982	0.0339	0.0300	0.0154
10	0.983	0.0521	0.0462	0.0237
20	0.963	0.0799	0.0708	0.0364
30	0.988	0.1360	0.1205	0.0619

Variation of k_d as a function of temperature is exponential (Fig. 4B) according to $k_d = 0.0285e^{0.0473 \times t}$. The adsorption constant $k_aQ°$ is obtained as: $k_dK_p = k_d \times 0.514$. Schematically the kinetics constants increase by a factor of about 1.6 for every 10 Celsius degree increase.

4.2.3. Activation energy and adsorption process

According to the Arrhenius law, k_d can be expressed as:

$$k_d = Ae^{-\frac{E_a}{RT}}$$

with A = Arrhenius factor, E_a = activation energy (J mol^{-1}), R = universal gas constant (8.314 J mol^{-1} K^{-1}) and T = absolute temperature (K).

The activation energy for phosphate sorption in our experiments was obtained by plotting $\ln(k_d) = \ln(A) - Ea/RT$ vs $1/T$ (Fig. 5). The value found for E_a (product of the slope by R, after sign changed), was: E_a = 32.65 kJ mol^{-1}.

315

316 ## 5. DISCUSSION

317 ### 5.1. Kinetics constants at 20°C

318 Desorption of phosphate from sediment approaching an apparent equilibrium after about 25 hours is in
319 agreement with previously published results on phosphate desorption from soils (Vaidyanathan and Talibudeen,
320 1970). Unfortunately, despite a wide literature search, no desorption rate constant value could be found for
321 sediments into water. Shariatmadari et al. (2006) used the first order model to describe P release from Iranian
322 calcareous soils amended with a phosphate solution (about 1 µmol g^{-1}) for 1 month before desorption in $CaCl_2$
323 solutions. They report desorption rate constants from 0.0388 to 0.0611 h^{-1}, in the same range as our values
324 (0.057 h^{-1} to 0.128 h^{-1}), but the different methodologies may affect the results and bias the comparison.

325 Our data highlight that coastal sediments are able to release half their exchangeable phosphate in a few
326 hours in a water devoid of phosphate. Almost total consumption of phosphate is frequent in coastal water during
327 spring and summer after phytoplankton blooms. In these environments the high dynamic conditions due to tides
328 contribute to the resuspension of superficial bottom sediments which are a potential source of phosphate.
329 Overlooking this compartment would be a major gap in ecological models of coastal waters (Baretta et al,1995)
330 mainly with the increasing storm frequency (Garnier et al., 2018), intensity and duration (Stockwell et al., 2019)
331 which could increase resuspensions events ((Tammeorg et al., 2013).

332 Most studies dealing with phosphorus in sediments focus on the amount of phosphorus liable to be
333 retained on the sediment as a phosphate reservoir, but not on the kinetics of the process. The rare adsorption rate
334 constants we found were obtained in experimental conditions very different of ours. In a study by Tang et al.
335 (2014), sediments of a drinking water reservoir in China were loaded with phosphate solutions, but at sediment
336 and phosphorus concentrations up to one hundred times greater than ours. Additionally, our experiments show
337 that a reliable adsorption rate constant k_a cannot be obtained from the Langmuir equation. Although this problem
338 can be overcome by using the operational combined constant k_aQ°. the latter cannot be compared with other
339 literature values.

340 In our study, we selected sediments with differing grain sizes since the nature of particles may affect
341 surface interactions with phosphate and modify the exchange rates with surrounding water. The relationship
342 between the rate constants and the proportion of fine particles (< 63 µm) was thus examined (Fig.6).

For k_d, lower constants are generally associated with higher concentrations of fine particles (Fig. 6A). The slope of the linear regression (R^2 = 0.40) is significant at the 95 % confidence level with a p-value of 0.036. However, the variation over the whole range of proportion of fine particles remains narrow with a mean (± s) of 0.085 ± 0.023 h^{-1}. The combined adsorption constant k_aQ° appears independent of the sediment grain size (Fig. 6B), with a p-value of 0.99 for the regression slope and a mean (± s) of 0.028 ± 0.011 h^{-1}. Consequently, the mean values could be an acceptable choice for models in a first approach.

The quasi-independence of rate constants with the proportion of fine particles suggests that these particles exhibit the main interaction with phosphate whatever the amount of the coarse fraction of the sediment.

5.2. Temperature effect on rate constants

Estuarine and coastal waters are subjected to marked water temperature oscillations in diurnal and seasonal cycles. For example, in the Bay of Seine, our studies show that temperature varies from 5-6 °C in winter to 16-17 °C in summer. Because of the high dynamics induced by the tide, the water is almost homogeneous from surface to bottom, with no thermocline at any time. Bottom sediments resuspended in the water column are therefore submitted to higher temperatures in summer when water phosphate concentrations are depleted following phytoplankton growth.

Our experiments show an increase of the rate constants by a factor of 4 between 1 °C and 30 °C while the final phosphate concentration released from the sediment remains independent of temperature within a coefficient of variation of a few percents. A noticeable result is that the two rate constants k_a and k_d show similar variations in relation to temperature. Using the law of temperature dependence of the rates, deduced from the experiments, modeling phosphate dynamic exchanges between sediment and seawater becomes possible. This is a step forward beyond the concept of the sediment as a phosphate reservoir.

An additional result is that K_p determined at 20 °C is valid regardless of the temperature (range 1-30 °C). This simplifies the laboratory procedure if the ability of a sediment to exchange with surrounding water at any temperature should be inferred from sediment exchangeable phosphate and water phosphate concentration (Andrieux-Loyer and Aminot, 2023). Indeed, this allows a single IDE experiment to be performed at room temperature.

In this study, the determination of the magnitude of activation energy (E_a) can provide insight into the type of molecular bounds encountered (physical or chemical). According to Saha et al (2010) the activation

372 energy for physisorption is usually no more than 40 kJ mol^{-1} since the forces involved in physisorption are weak.
373 In their study, Inglezakisa and Zorpas (2012) found that most of their E_a values for physisorption are below the
374 higher limit of 40 kJ mol^{-1} found in literature, while the 24-40 kJ mol^{-1} range corresponds to ionic exchanges.

375 The value found for E_a was: E_a = 32.65 kJ mol^{-1}. This agrees with the above range for physisorption,
376 mainly governed by ionic mechanisms (Inglezakisa and Zorpas, 2012). For lake sediments, Topçu et al. (2018)
377 found E_a in the range 3-11 kJ mol^{-1} while the value of 48.5 kJ mol^{-1} was reported by Omari et al. (2019) using
378 sediments of a Morocco wadi (riverbed). The differences may be attributed to the sediment types but all values
379 remain lower or close to the 40 kJ mol^{-1} criterion below which physisorption is the dominant process.

380 ## 6. CONCLUSION

381 This work aimed to determine the kinetic behavior for the adsorption-desorption processes of phosphate on
382 coastal sediments. Relying on the Langmuir theory, adapted to solid-water exchanges in natural environments, it
383 was possible to determine the rate constants for adsorption and desorption processes. The desorption constant is
384 little influenced by sediment grain size with a RSD of only 27% over the whole range of fine fraction (0-100% <
385 63 µm) and the combined adsorption constant is independent of grain size. The variation of the rate constants in
386 relation to temperature was established in the range 1-30 °C showing that the rates increase approximately by a
387 1.6 factor for a 10 °C increase. Ionic physisorption of phosphate on coastal sediments agrees with our activation
388 energy results. The partition coefficient and the Langmuir constant (rate constants ratio) were independent of
389 temperature over the tested range. These results are essential to develop environmental models which need to
390 include the sediment phase as a contributor to phosphate cycling in estuarine and coastal systems.
391

392 **Acknowledgements** We thank Roger Kérouel, Xavier Philippon, Agnès Youenou, Anne Daniel-Scuiller,
393 Marie-Madeleine Danielou and Erwan Le Gall for their collaboration during the sampling surveys in the Bay of
394 Seine and the Penzé estuary and our colleagues working for the national monitoring network (Réseau National
395 d'Observation) for their help during the cruises in the Loire and Gironde estuaries. Roger Kérouel, brought
396 assistance for laboratory work. We are grateful to Yann Aminot for his constructive comments and for language
397 review.

398 **Author contributions** The two authors have participated in the research and article preparation (Study's
399 conception, acquisition of samples, phosphate analysis, writing of the manuscript).

Funding This work was partially funded by the research program PNOC (Programme National d'Océanographie Côtière) and by the project ICREW (Improving Coastal and Recreational Waters).

Data availability The data presented in the current study are available from the corresponding author upon request.

Conflict of interest The authors declare that they have no conflicts of interest.

References

Ait Ballagh FE, Rabouille C, Andrieux-Loyer F, Soetaert K, Elkalay K, Khalil K (2020) Spatio-temporal dynamics of sedimentary phosphorus along two temperate eutrophic estuaries: A data-modelling approach. Continental Shelf Research 193: 1-23.

Ait Ballagh FE, Rabouille C, Andrieux-Loyer F, Soetaert K, Lansard B, Bombled B, Monvoisin G, Elkalay K, Khalil K (2021) Spatial Variability of Organic Matter and Phosphorus Cycling in Rhône River Prodelta Sediments (NW Mediterranean Sea, France): a Model-Data Approach. Estuaries and Coasts 44(7): 1765-1789.

Aminot A, Andrieux F (1996) Concept and determination of exchangeable phosphate in aquatic sediments. Water Research 30: 2805-2811.

Aminot A, Kérouel R, Coverly SC (2009) Nutrients in seawater using segmented flow analysis. In: Wurl O (ed) Practical guidelines for the analysis of seawater. CRC Press, Boca Raton, pp 143–178.

Andrieux-Loyer, Aminot (2023) Assessing exchangeable phosphate and related data in coastal sediments: Theoretical and practical considerations. Estuarine, Coastal and Shelf Science 281: 108218.

Andrieux-Loyer F, Azandegbe A, Caradec F, Philippon X, Kerouel R, Youenou A, Nicolas JL (2014) Impact of oyster farming on Diagenetic Processes and the Phosphorus Cycle in Two Estuaries (Brittany, France). Aquatic Geochemistry 20(6): 573-611

Baretta JW, Ebenhöh W, Ruardij P (1995) The European regional seas ecosystem model, A complex marine ecosystem model. Netherlands Journal of Sea Research 33(3/4): 233-246.

Boesch DF (2002) Challenges and opportunities for science in reducing nutrient over-enrichment of coastal ecosystems. Estuaries 25:744-758.

Cha HJ, Lee CB, Kim BS, Choi MS, Ruttenberg KC (2005) Early diagenetic redistribution and burial of phosphorus in the sediments of the southwestern East Sea (Japan Sea). Marine Geology 216: 127-143.

Couceiro F, Fones GR, Thompson CEL, Statham PJ, Sivyer DB, Parker R, Kelly-Gerreyn BA, Amos CL (2013) Impact of resupension of cohesive sediments at the Oyster Grounds (North Sea) on nutrient exchange across the sediment-water interface. Biogeochemistry 113: 37-52.

Garnier E, Ciavola P, Spencer T, Ferreira O, Armaroli C, McIvor A (2018) Historical analysis of storms events: Cases studies in France, England, Portugal and Italy. Coastal Engineering 134: 10-23.

Inglezakisa VJ, Zorpas AA (2012). Heat of adsorption, adsorption energy and activation energy in adsorption and ion exchange systems in Desalination and Water Treatment 39:149–157·

Jarvies HP, Withers JA, Neal C (2002). Review of robust measurement of phosphorus in river water: sampling, storage, fractionation and sensitivity. Hydrology and Earth System Sciences Discussions, European Geosciences Union 6(1):113-131.

Li M, Whelean MJ, Wang GQ, White SM (2013) Phosphorus sorption and buffering mechanisms in suspended sediments from the Yangtze Estuary and Hangzhou Bay, China. Biogeosciences 10:3341-3348.

Murphy J, Riley JR (1962) A modified single solution method for the determination of phosphate in natural waters. Analytica Chimica Acta 27:31-36.

Omari H, Dehbi A, Lammini A, Abdallaoui A (2019) Study of the Phosphorus Adsorption on the Sediments. Journal of Chemistry 2019: ID 2760204, 10 pages

Otero M, Coelho JP, Rodrigues ET, Pardal MA, Santos EBH, Esteves VI, Lille

bo AI (2013) Kinetics of the PO4-P adsorption onto soils and sediments from the Mondego estuary (Portugal). Marine Pollution Bulletin 77:361-366.

Saha P, Chowdhury S, Gupta S, Kumar I (2010) Insight into adsorption equilibrium, kinetics and thermodynamics of Malachite Green onto clayey soil of Indian origin. Chemical Engineering Journal 165: 874-882.

Seitzinger SP, Harrison JA, Dumont E, Beusen AHW, Bouwman A.F (2005) Sources and delivery of carbon, nitrogen, and phosphorus to the coastal zone: An overview of Global Nutrient Export from Watersheds (NEWS) models and their application. Global Biological Cycles 19(4): GB4S01.

Shariatmadari H, Shirvani M, Jafari A (2006) Phosphorus release kinetics and availability in calcareous soils of selected arid and semiarid toposequences. Geoderma 132: 261-272.

Smil V (2000) Phosphorus in the environment: natural flows and human interferences. Annual Review of Energy Environment 25:53–88.

Sondergaard, Kristensen P, Jeppesen E (1992) Phosphorus release from resuspended sediment in the shallow and wind-exposed Lake Arreso, Denmark. Hydrobiologia 228: 91-99.

Stockwell JD, Doubek JP, Adrian R, Anneville O, Carey CC, Carvalho L, De Senerpont Domis LN, Dur G, Frassl MA, Grossart H-P, Ibelings BW, Lajeunesse MJ, Lewandowska AM, Llames ME, Matsuzaki SS, Nodine ER, Nõges P, Patil VP, Pomati F, Rinke K, Rudstam LG, Rusak JA, Salmaso R, Seltmann CT, Straile D, Thackeray SJ, Thiery W, Urrutia-Cordero P, Venail P, Verburg P, Woolway RI, Zohary T, Andersen MR, Bhattacharya R, Hejzlar R, Janatian N, Kpodonu ATNK, Williamson TJ, Wilson HL (2019) Storm impacts on phytoplankton community dynamics in lakes. Global Change Biology 26 (5): 2756-2784.

Tammeorg O, Niemistö J, Möls T, Laugaste R, Panksep K, Kangur K (2013) Wind-induced sediment resuspension as a potential factor sustaining eutrophicationin large and shallow Lake Peipsi. Aquatic Science 75: 559-570.

Tang X, Wu M, Dai X, Chai P (2014) Phosphorus dynamics and adsorption characteristics for sediment from a drinking water source reservoir and its relation with sediment compositions. Ecological Engineering 64:276-284.

Topçu A, Ulusoy U, Pulatsü S (2018) Determination of sediment phosphate sorption characteristics in shallow Mogan lake, Turkey. Applied Ecology and Environmental Research 16(5): 5971-5985.

Van Raaphorst W, Kloosterhuis HT (1994) Phosphate adsorption in superficial intertidal sediments. Marine Chemistry 48:1-16.

Vaidyanathan LV, Talibudeen O (1970) Rate processes in the desorption of phosphate from soils by ion-exchange resins. Journal of Soil Science 21(1): 173-183.

Wang X, Zhang L, Zhang H, Wu X, Mei D (2012) Phosphorus adsorption characteristics at the sediment–water interface and relationship with sediment properties in FUSHI reservoir, China. Environmental Earth Sciences 67: 15-22.

Wang S, Vogt RD, Carstensen J, Lin Y, Feng J, Lu X (2022) Riverine flux of dissolved phosphorus to the coastal sea may be overestimated, especially in estuaries of gated rivers: Implications of phosphorus adsorption/desorption on suspended sediments. Chemosphere 287: 132206.

Voice TC, Weber WJJr (1983) Sorption of hydrophobic compounds by sediments, soils and suspended solis-I. Theory and backgtound. Water Research 17(10): 1433-1441.

Zhang B, Fang F, Guo JS, Chen YP, Li Z, Guo SS (2012) Phosphorus fractions and phosphate sorption-release characteristics relevant to the soil composition of water-level-fluctuating zone of Three Gorges Reservoir. Ecological Engineering 40: 153-159.

Zhou A, Tang H, Wang D (2005) Phosphorus adsorption on natural sediments: Modeling and effects of pH and sediment composition. Water Research 39: 1245-1254

Figure captions

Fig. 1. Comparison of kinetics performed on sediments freshly treated and treater after lyophilisation. Two sediments from the Bay of Seine with different exchangeable phosphate concentrations were used.

Fig. 2. A: Kinetics experiment performed with the sediment from station 17 of the Bay of Seine (S = 0.2 g L^{-1}); B: Determination of the desorption rate constants (k_d) by plotting $\ln(q_{Re}/(q_{Re} - q_{Rt}))$ versus time;

$k_d = slope \times (q_{Re}/q_i)$

Fig. 3. Release of phosphate from the same sediment (Bay of Seine, station 16), at increasing temperatures (note the two time scales)

Fig. 4. A: logarithmic functions of kinetics of phosphate release as a function of time. B: variation of the adsorption constant k_d as a function of temperature.

Fig. 5. Plot of $\ln(k_d)$ versus $1/T$ for estimation of activation energy (E_a; kJ mol^{-1})

Fig. 6. A: Distribution of the desorption constant k_d and B: the combined adsorption constant $k_a Q^o$ (= $k_d K_p$) as a function of the < 63 µm sediment fraction, in selected sediments covering this fine fraction range.

Table captions

Table 1 Nomenclature used herein

Table 2 Results of desorption rate constant (k_d) determination obtained from the kinetic experiments according to the function described in Section 2.2.2

Table 3 Results of adsorption rate constants (k_a and $k_aQ°$) determinations

Table 4 Final and computed equilibrium concentrations at the various temperatures

Table 5 Results of rate constants (k_d, k_a and $k_aQ°$) obtained at various temperatures. Common main data: S = 0.25 g L^{-1}; q_i (= exch-P) = 2.46 µmol g^{-1}; q_{Re} = 2.18 µmol g^{-1}; K_p = 0.514 L g^{-1}

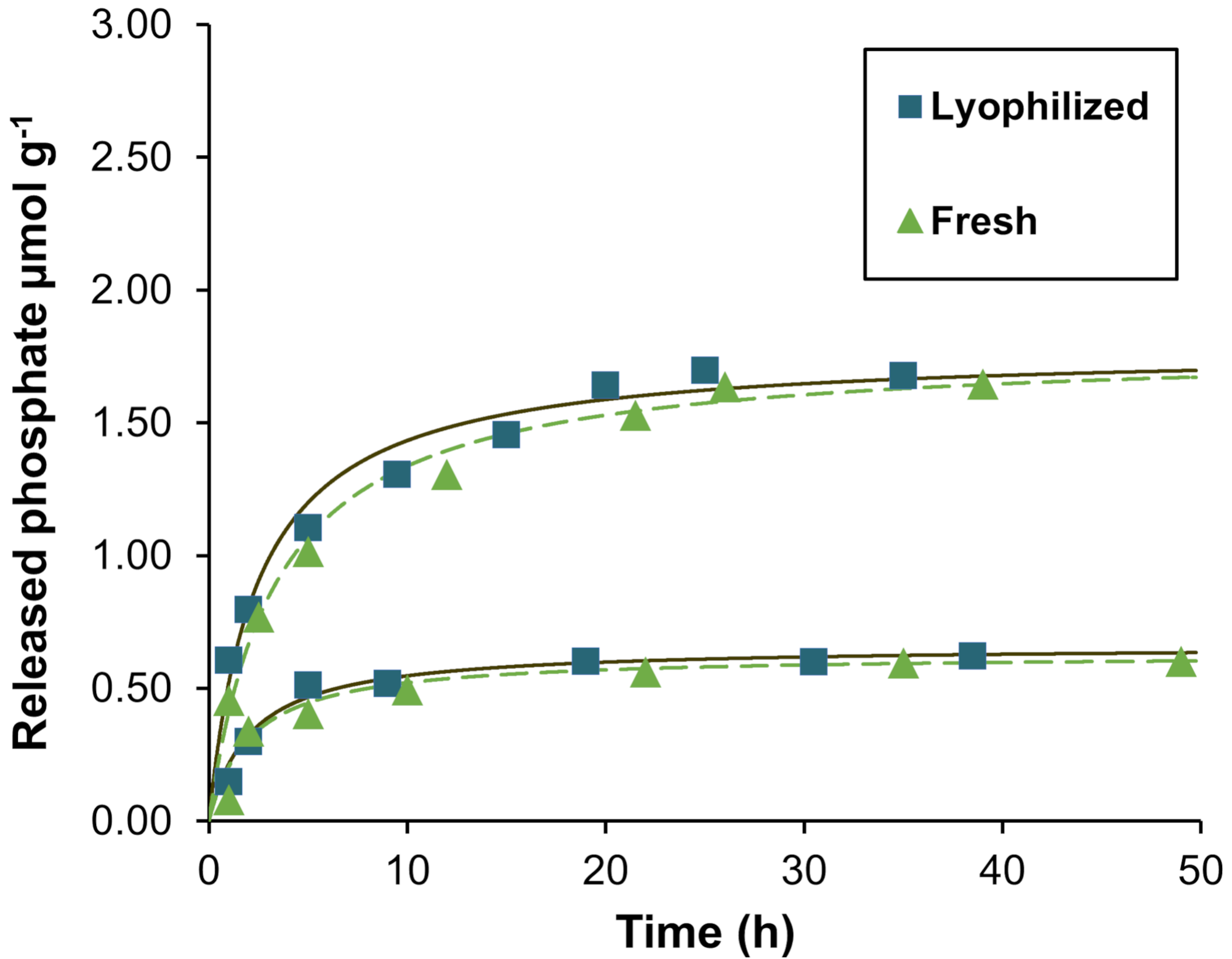
Released phosphate µmol g-1
3.00
2.50
2.00
1.50
1.00
0.50
0.00
0
10
20
30
40
50
Time (h)
Lyophilized
Fresh

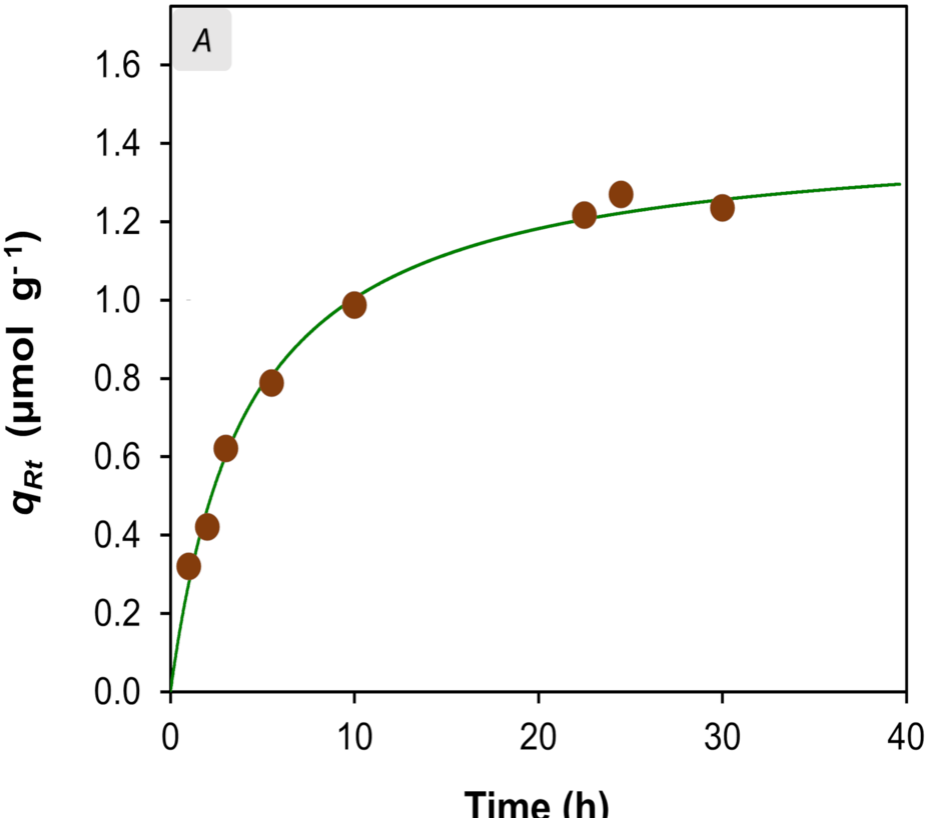
A
1.6
1.4
1.2
1.0
0.8
0.6
0.4
0.2
0.0
0
10
20
30
40
q_{Rt} (µmol g^{-1})
Time (h)

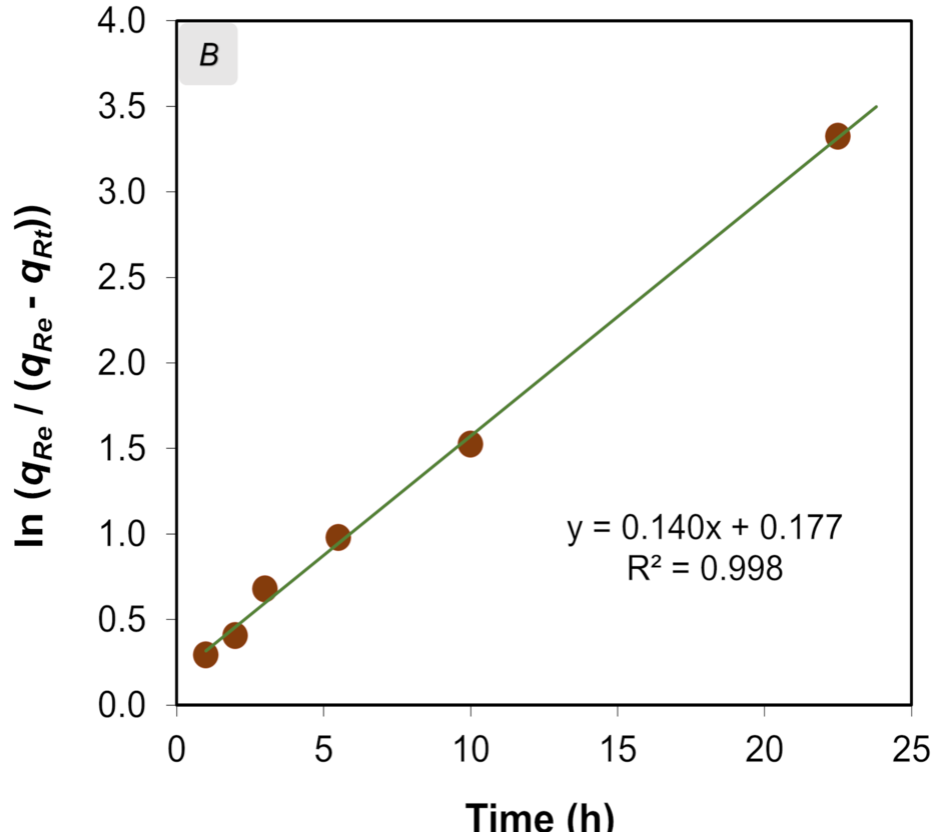
B
4.0
3.5
3.0
2.5
2.0
1.5
1.0
0.5
0.0
0
5
10
15
20
25
ln (q_{Re} / (q_{Re} - q_{Rt}))
y = 0.140x + 0.177
R² = 0.998
Time (h)

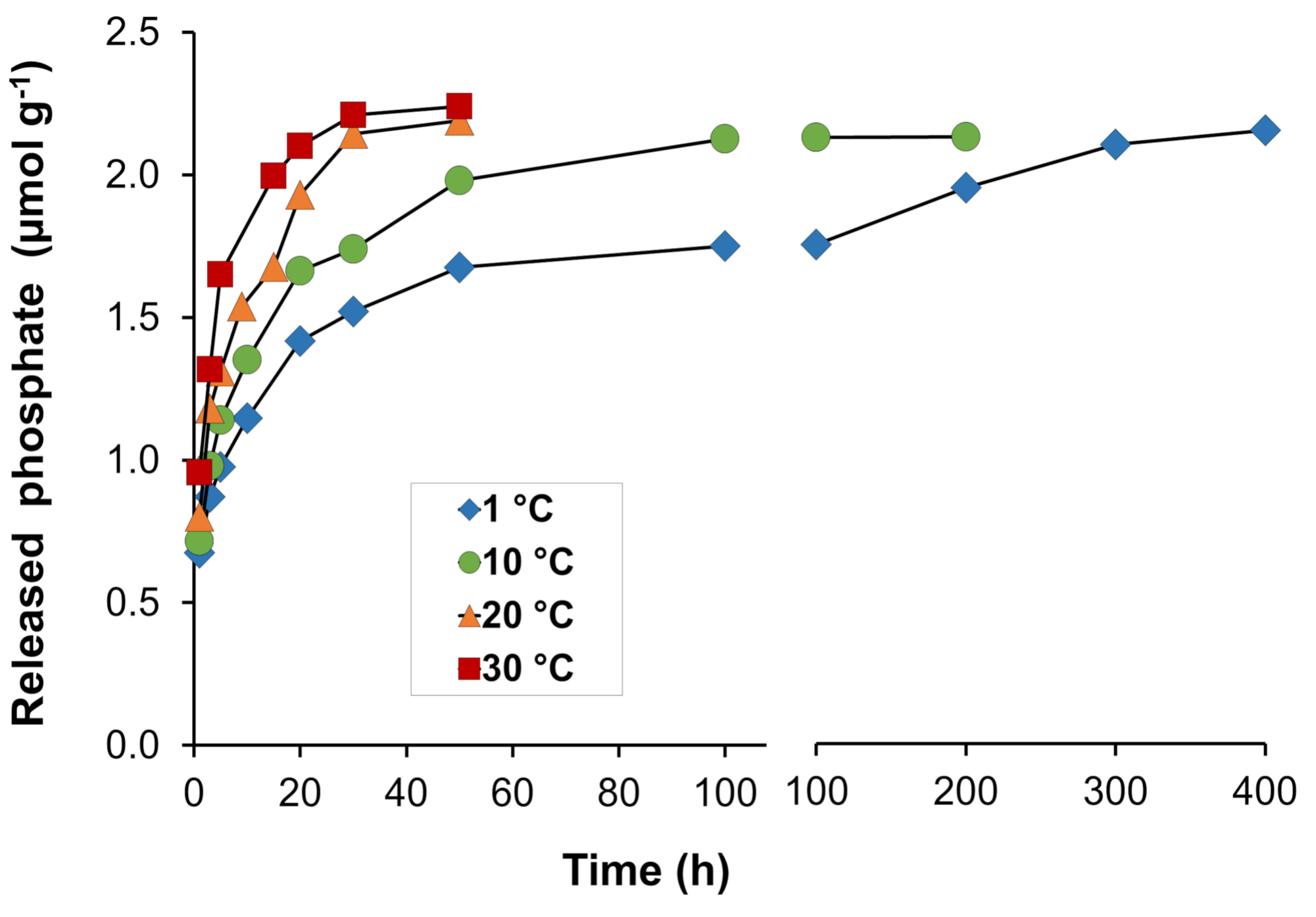
Released phosphate (µmol g-1)
2.5
2.0
1.5
1.0
0.5
0.0
0
20
40
60
80
100
100
200
300
400
Time (h)
1 °C
10 °C
20 °C
30 °C

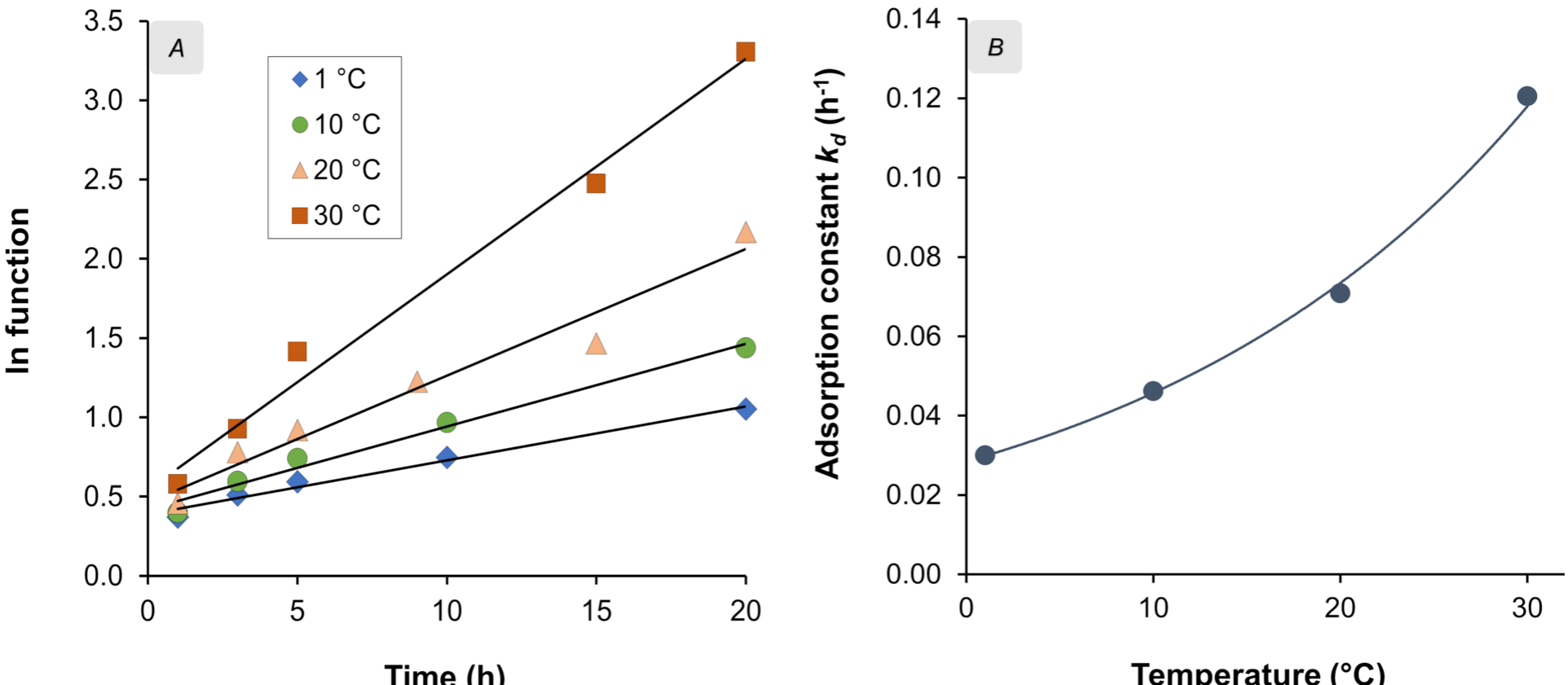
A
1 °C
10 °C
20 °C
30 °C
ln function
Time (h)
0.0
0.5
1.0
1.5
2.0
2.5
3.0
3.5
0
5
10
15
20
B
Adsorption constant k_d (h^{-1})
Temperature (°C)
0.00
0.02
0.04
0.06
0.08
0.10
0.12
0.14
0
10
20
30

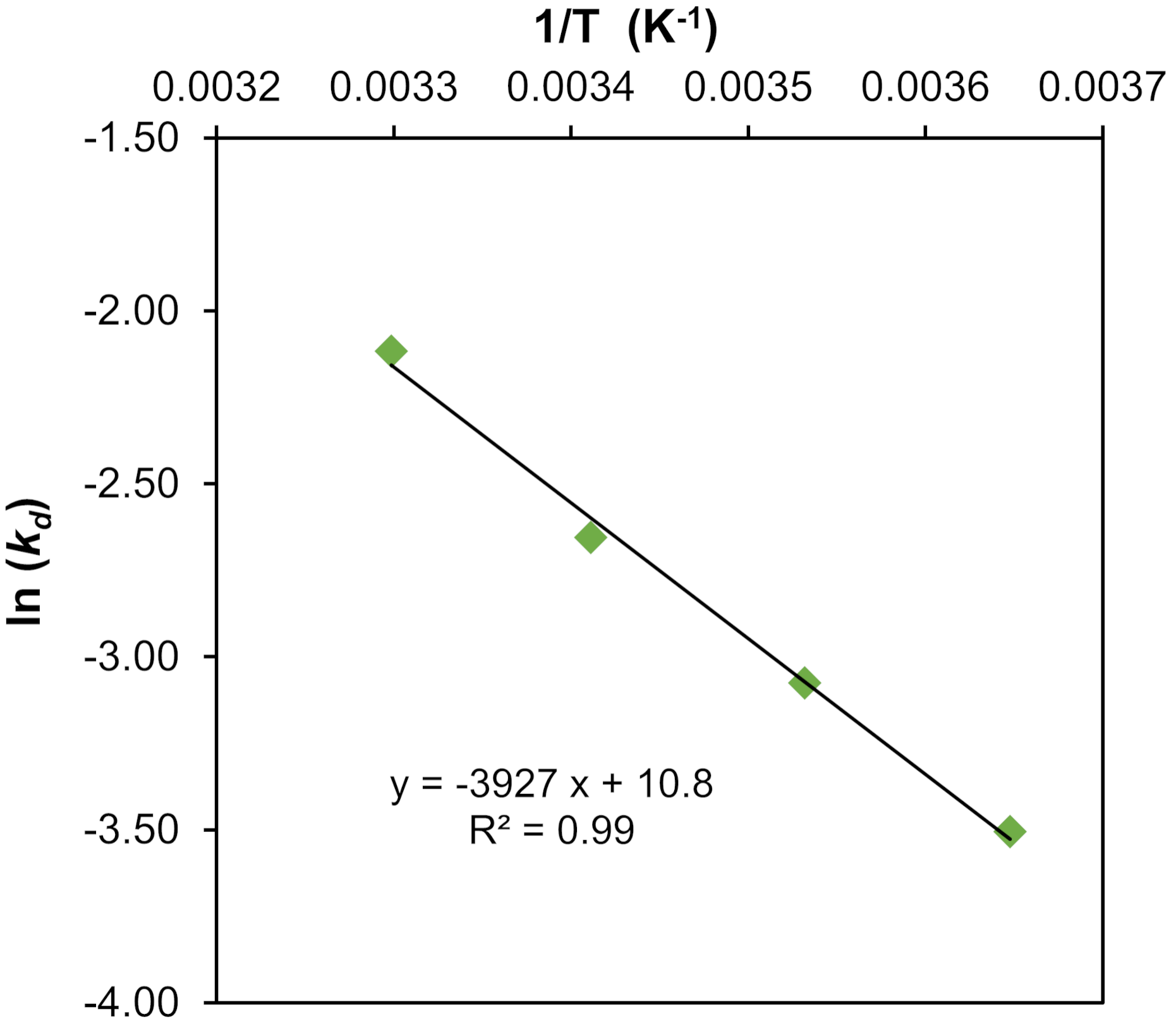
1/T (K-1)
0.0032
0.0033
0.0034
0.0035
0.0036
0.0037
-1.50
-2.00
-2.50
-3.00
-3.50
-4.00
ln (kd)
y = -3927 x + 10.8
R² = 0.99

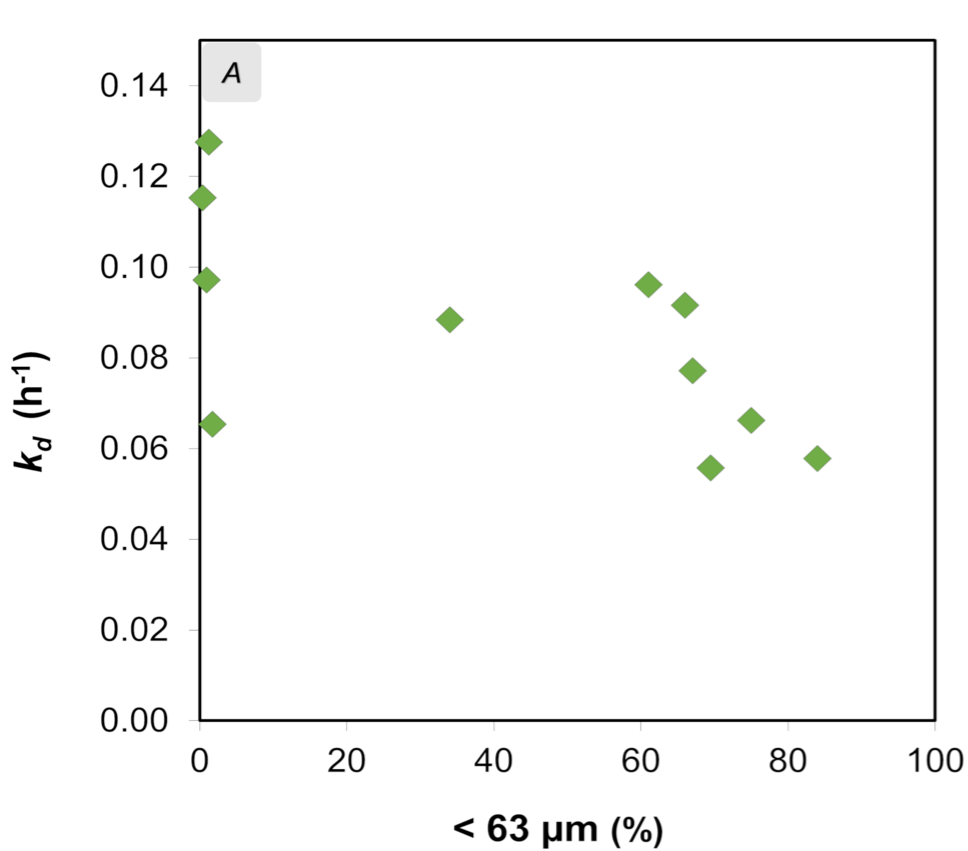
A
0.14
0.12
0.10
0.08
0.06
0.04
0.02
0.00
k_d (h^{-1})
0
20
40
60
80
100
< 63 µm (%)

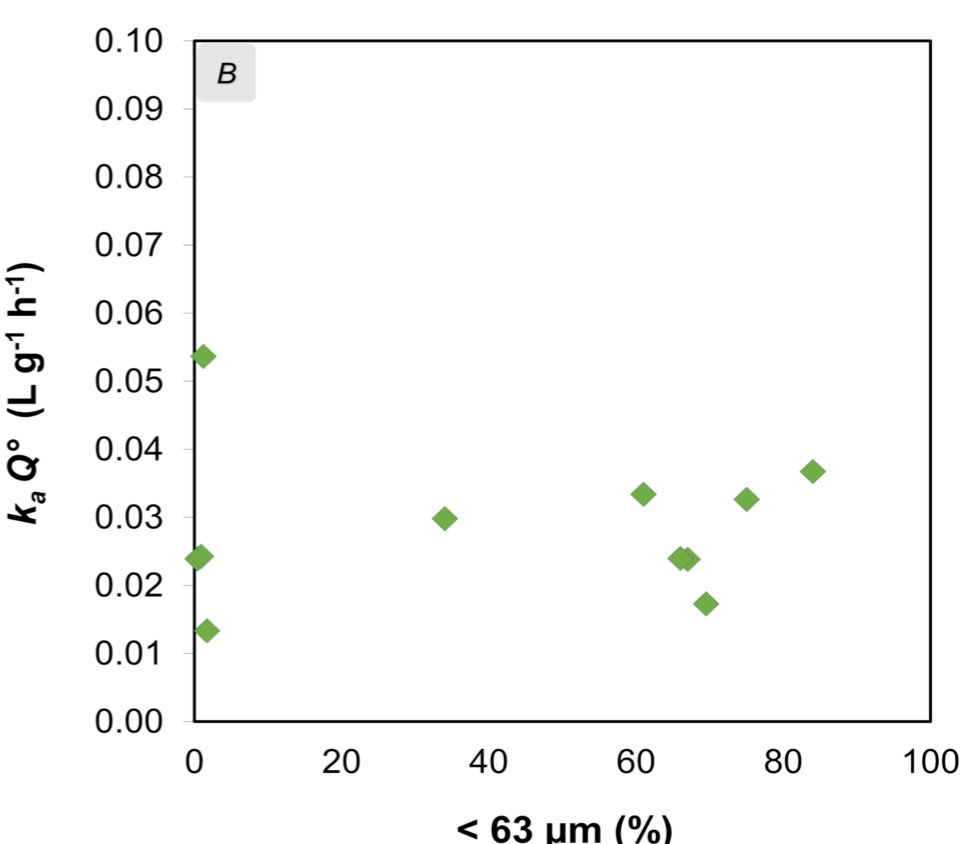
B
0.10
0.09
0.08
0.07
0.06
0.05
0.04
0.03
0.02
0.01
0.00
$k_a Q°$ (L g^{-1} h^{-1})
0
20
40
60
80
100
< 63 µm (%)

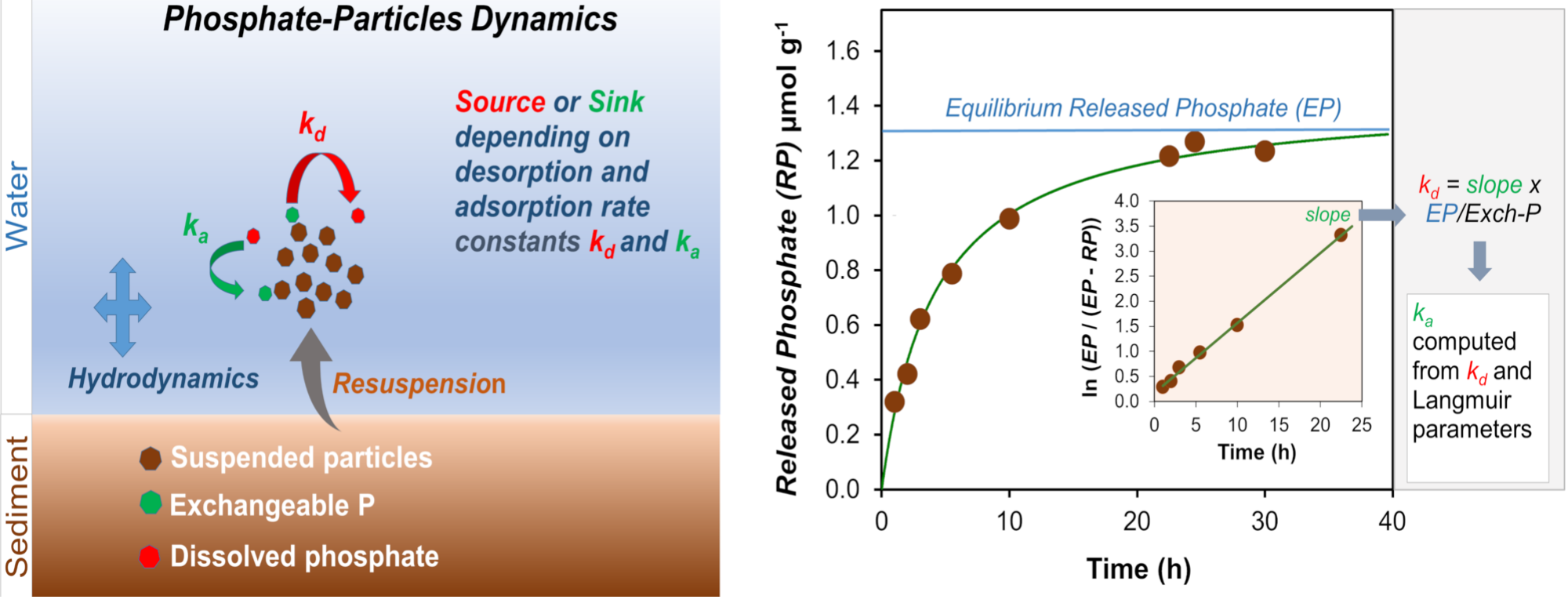
Phosphate-Particles Dynamics
Water
Sediment
Source or Sink depending on desorption and adsorption rate constants k_d and k_a
k_d
k_a
Hydrodynamics
Resuspension
Suspended particles
Exchangeable P
Dissolved phosphate
Released Phosphate (RP) µmol g^{-1}
Equilibrium Released Phosphate (EP)
Time (h)
ln (EP / (EP - RP))
slope
k_d = slope x EP/Exch-P
k_a computed from k_d and Langmuir parameters